

*Short Communication*

## **Shifts in the Binding Energies of Cr2p, Fe2p and O1s electrons of Alloy Oxide Films in the Presence of Pb During High-Temperature Water Corrosion**

*Shenghan Zhang, Quan Lu, Hao Zhang, Kexin Liang, Yu Tan\*, Chenhao Sun*

Department of Environment Science and Engineering, North China Electric Power University, Baoding 071003, P.R. China

\*E-mail: [lucifertan@163.com](mailto:lucifertan@163.com)

*Received: 29 June 2019 / Accepted: 15 October 2019 / Published: 31 December 2019*

---

Pb (lead) in high-temperature pressurized water of a PWR secondary circuit may cause stress corrosion cracking in stainless steel and Ni-based alloys. A simulated primary circuit environment of PWR was employed to form an oxide film on stainless steel 304 and Incoloy 800 and investigate high-temperature water corrosion with trace additions of Pb. The morphology of the alloy surfaces suggested differences in whether protective spinel oxides or ineffective scaly oxides were formed with trace additions of Pb. The binding energies of chromium, iron and oxygen of the alloy oxide films were shifted to lower energies by Pb addition as verified from an XPS analysis.

---

**Keywords:** lead; PWR-type reactor; stainless steel; water chemistry

### **1. INTRODUCTION**

A steam generator for a pressurized water reactor (PWR), which works as the barrier between the primary circuit and secondary circuit, was constructed with stainless steel and Ni-based alloys. Incoloy 800 is employed for its outstanding anti-corrosion and anti-SCC (stress cracking corrosion) properties with a balanced ratio of Fe:Cr:Ni as the tube material of the steam generator[1]. Until now, there has been no failure report of Incoloy 800 for SCC. Lead (Pb) is a neutron absorber with the advantages of a low absorption interface and little ability to slow neutrons while remaining an SCC-sensitive material to iron-based materials, such as stainless steel and Ni-based alloys, in a high-temperature pressurized water environment. In addition, the primary circle of a PWR may be easily polluted by lead as a result of the water supply, welding work, start and stop processes or other factors. Previous studies [2-6] have indicated that Pb induces the SCC (PLSCC) of alloys in high-temperature pressurized water. The concentrations of lead added in the above studies are well over the possible lead

concentration level in actual operation conditions, such as 500 ppm or even 10,000 ppm, in addition to stringent conditions such as a pH 12.7 or pH 1.5. These previous studies focused mainly on the impact of the mechanical properties of the alloy by PLSCC.

In this paper, a simulated neutral aqueous solution with Pb was employed to investigate the various energy shifts of the metal bands by X-ray photoelectron spectroscopy (XPS) for long-term high-temperature water corrosion, in addition to the corrosion behaviour and morphologies of the alloy oxide films. Typical nuclear-grade stainless steel 304 (SS304) and Incoloy 800 are introduced for this research.

## 2. EXPERIMENTAL

The chemical compositions of SS304 and Incoloy 800 used in this work are listed in Table 1. Coupons (12.0\*10.0\*3.0 mm) were mechanically polished with SiC papers up to 2000 grit and then finished with 0.3  $\mu\text{m}$  alumina gel. Next, the specimens were first cleaned in distilled water and then in ethanol by an ultrasonic machine. After cleaning, they were kept in a dry box.

**Table 1.** Chemical compositions of SS304 and Incoloy 800 mass fraction (wt%)

Alloys	C	Si	Mn	P	S	Ni	Cr	Mo	Fe
SS304	0.016	0.66	1.66	0.032	0.005	10.39	18.57	-	balance
Incoloy 800	0.08	0.3	0.9	-	0.000	30.5	19.8	-	47.3

As discussed [7-8], high-temperature water contained 2 ppm lithium hydroxide (denoted  $\text{Li}^+$ ), 500 ppm boric acid and 200 ppb  $\text{Co}^{2+}$  with additions of 10, 20, 50, and 100 ppb  $\text{PbO}$ . A  $\text{PbO}$ -free solution was also prepared. Each set of specimens was placed into an autoclave and oxidized in the above solution for 100 h at 315°C.

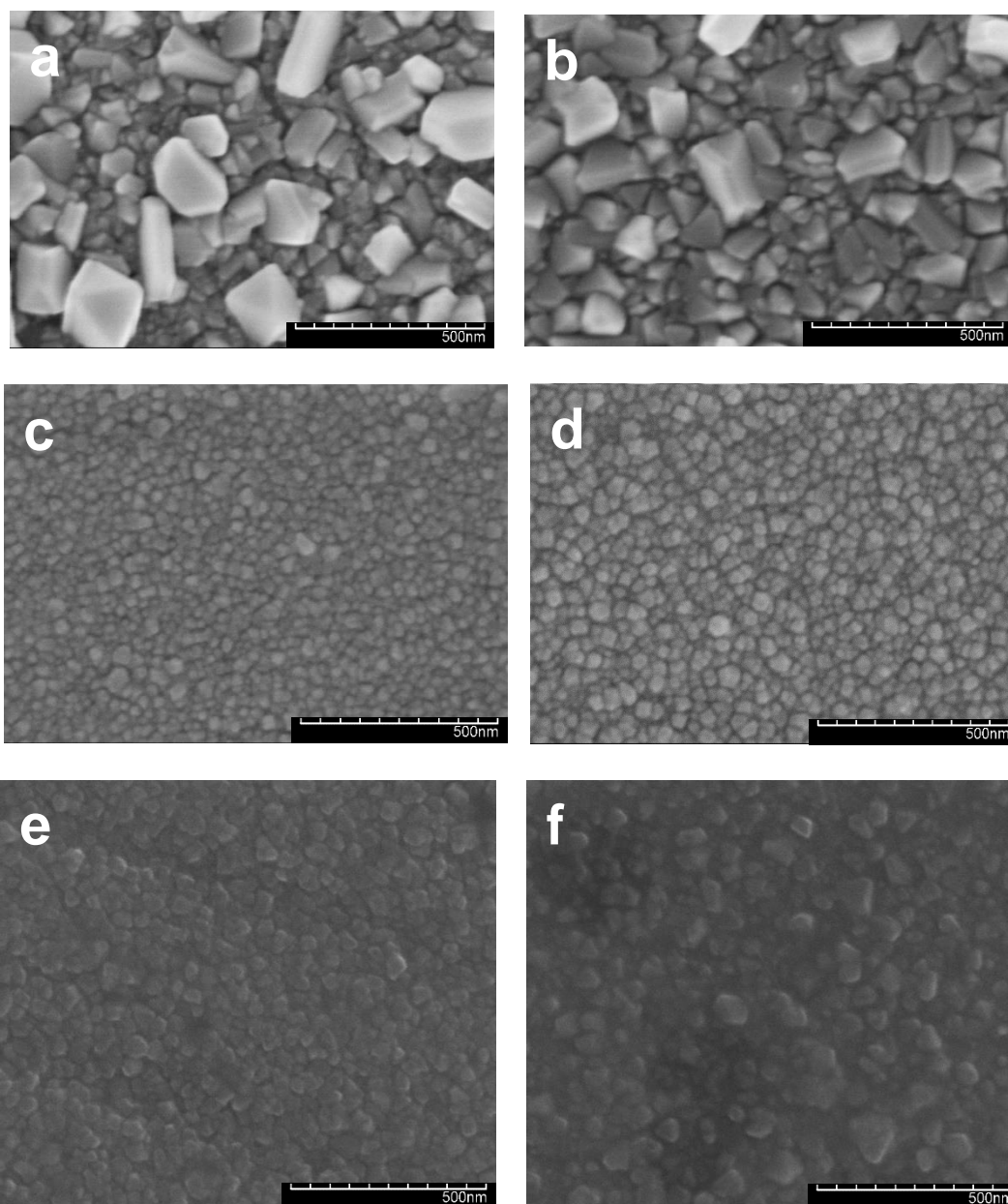
A conventional three-electrode cell was employed in these experiments. A saturated calomel electrode (SCE) was used as the reference electrode, and a platinum electrode was used as the counter electrode. All experiments were carried out at room temperature (25°C). The supporting solution used in the electrochemical measurements contained 0.15  $\text{mol}\cdot\text{L}^{-1}$  boric acid and 0.0375  $\text{mol}\cdot\text{L}^{-1}$  sodium borate buffer (pH = 8.4). Before testing, the solution was de-aerated with pure nitrogen gas for 1 h, which was then continued throughout the experiment. The electrochemical measurements were performed using a PARSTAT 2273 potentiostat. The potentiodynamic polarization usually started from 0.2 V below the open circuit potential (OCP) and scanned to the designated positive potential with a scanning rate of 1.0 mV/s.

## 3. RESULTS

### 3.1. Morphologies of oxide films changed by $\text{PbO}$

Fig. 1 shows the FESEM images of the oxide films on the alloys after high-temperature water oxidation. The surface of Incoloy 800 with no  $\text{PbO}$  addition (Fig. 1a) was covered by typical oxide

particles: a sparse number of large particles, a dense agglomeration of smaller ones and a few unique particles, such as needles for Co and its oxide. When 10 ppb PbO was added into the water, as shown in Fig. 1b, the oxide particles decreased in size. When the PbO concentration increased to 20 ppb (Fig. 1c), the typical oxide particles disappeared with ‘ulcerous’ corrosion products instead. This ulcerous corrosion product increased in size when the PbO concentration increased to 50 ppb (Fig. 1d). Similarly, Fig. 1e-h show the surface morphologies of the SS304 oxide film after high-temperature water oxidation at different concentrations of PbO.



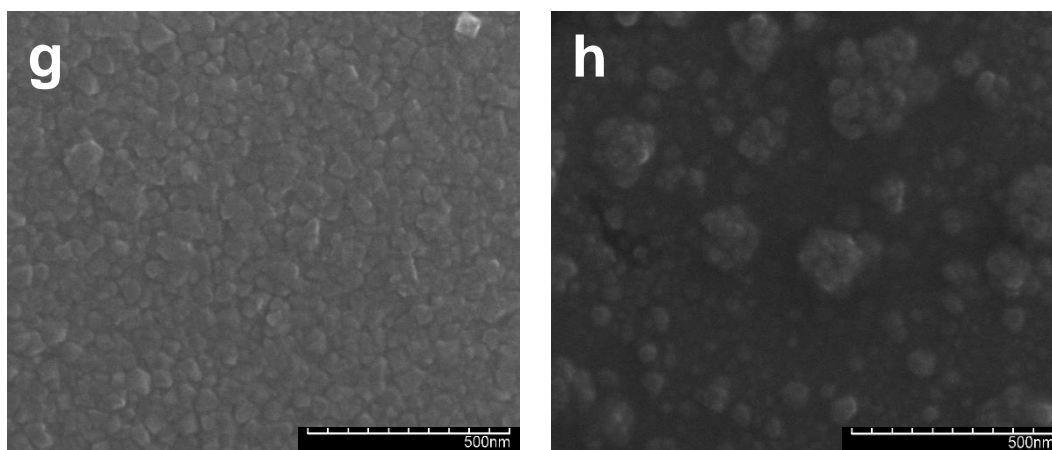


**Figure 1.** SEM images of the oxide film surface for Incoloy 800 after corroding in solutions with (a) 0, (b) 10, (c) 20, and (d) 50 ppb PbO additions and that of stainless steel 304 corroded in solutions with (e) 0, (f) 10, (g) 50, and (h) 100 ppb PbO additions for 120 h at 315°C.

The surface of the PbO-free sample (Fig. 1e) was covered with typical metal oxides. Some oxides shrank/disappeared when PbO increased to a concentration of 10 ppb (Fig. 1f) or 50 ppb (Fig. 1g). When PbO in high-temperature water increased to 100 ppb, a number of ulcerative corrosion products could be found.

### 3.2 Potentiodynamic polarization

The potentiodynamic polarization results of the Incoloy 800 specimens oxidized in high-temperature water with various amounts of PbO additions are plotted in Fig. 2a. Furthermore, an inset figure is plotted and fitted to suggest the Tafel region and current densities of different oxide films on Incoloy 800. The polarization plot of 0 ppb PbO indicated a typical plot as a non-aggressive solution with a current density of  $-8.41$  ( $\log(\text{A}\cdot\text{cm}^{-2})$ ). With the addition of 10 ppb PbO into the high-temperature water, the polarization plot of the oxide film indicated a lower current density ( $-8.49$   $\log(\text{A}\cdot\text{cm}^{-2})$ ) than that of 0 ppb PbO, and the plot of that with 20 ppb PbO indicated the same trend, with a much lower current density ( $-9.56$   $\log(\text{A}\cdot\text{cm}^{-2})$ ) than 10 ppb PbO. When the addition increased to 50 ppb, the polarization current increased ( $-8.72$   $\log(\text{A}\cdot\text{cm}^{-2})$ ), but it was still lower than that of the 0 ppb PbO addition. Moreover, the different corrosion potentials indicated a positive movement from the addition of 0 to 20 ppb PbO. The PbO addition into the high-temperature water had an impact on the oxidation properties of the film on Incoloy 800, as shown in the results.

Additionally, the polarization curves of SS304L specimens show corrosion occurs in high-temperature water with various PbO treatments as shown in Fig. 2b.

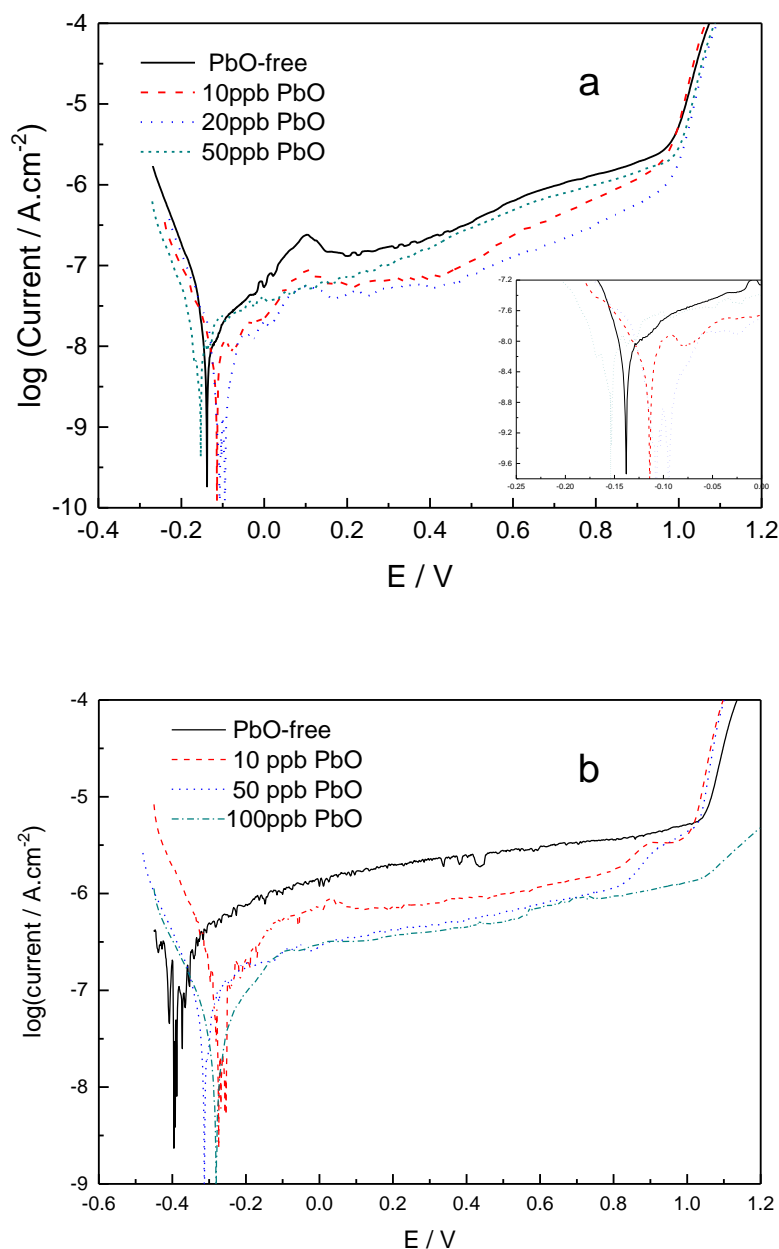


**Figure 2.** Potentiodynamic polarization curves of the (a) Incoloy 800 and (b) SS304 specimens after high-temperature water oxidation with various amounts of PbO at a polarization rate of  $1 \text{ mV}\cdot\text{s}^{-1}$ .

### 3.3 XPS of the oxide film on SS304 with PbO addition

To study the effect of trace PbO in high-temperature water on the composition and material phase of the metal oxide on SS304, the XPS results were deconvoluted by a peak fitting process, as shown in Fig. 3. The first column indicates the C1s spectrum of the oxide film formed by the PbO-free specimen and the 50 ppb PbO addition at the same peak position (284.8 eV). Columns 2, 3 and 4 indicate the spectra of Cr2p3/2, Fe2p3/2 and O1s of the oxide film with 50 ppb PbO (c, e and g) and with the PbO-free oxide film (b, d and f), respectively. In the case of the Cr2p3/2 peaks for the PbO-free oxide film

(b0, b1:0 at the surface, 1 as the Ar<sup>+</sup> was sputtered for 80 s), the binding energies of Cr<sup>0</sup>, Cr<sup>3+</sup> and Cr(OH)<sub>3</sub> were as follows: 574.2, 576.5 and 577.5 eV[9-12], respectively. Usually, Cr<sup>3+</sup> is considered to be a Cr<sub>2</sub>O<sub>3</sub> and chromium-rich spinel oxide corresponding to the metal oxide. It should be highlighted that when there is 50 ppb PbO added to the high-temperature water, the binding energy of Cr2p3/2 is shifted by ~0.3-0.5 eV in the direction of low electron energy as follows: Cr<sup>0</sup>, Cr<sup>3+</sup> and Cr(OH)<sub>3</sub> corresponding to 573.9, 576.0 and 577.1 eV, respectively. Similarly, the binding energies of Fe<sup>0</sup>, Fe<sup>2+</sup> and Fe<sup>3+</sup> were 706.8, 708.6 and 711.2 eV[10, 13] for the Fe2p3/2 fitting result with the PbO-free oxide film (d0, d1). The results suggested that Fe(OH)<sub>3</sub>, an iron-rich spinel oxide (Fe<sub>3</sub>O<sub>4</sub> and NiFe<sub>2</sub>O<sub>4</sub>), and Fe<sub>2</sub>O<sub>3</sub> and FeO were on the surface of the SS304 oxide film after high-temperature water oxidation. Although there is no evidence that the addition of trace level PbO changes the crystal composition of SS304, similar to the chromium analysis result, the binding energies of Fe2p3/2 in the oxide film also shifted in the low electron energy direction (~0.2-0.3 eV) with a 50 ppb PbO addition in the high-temperature water.

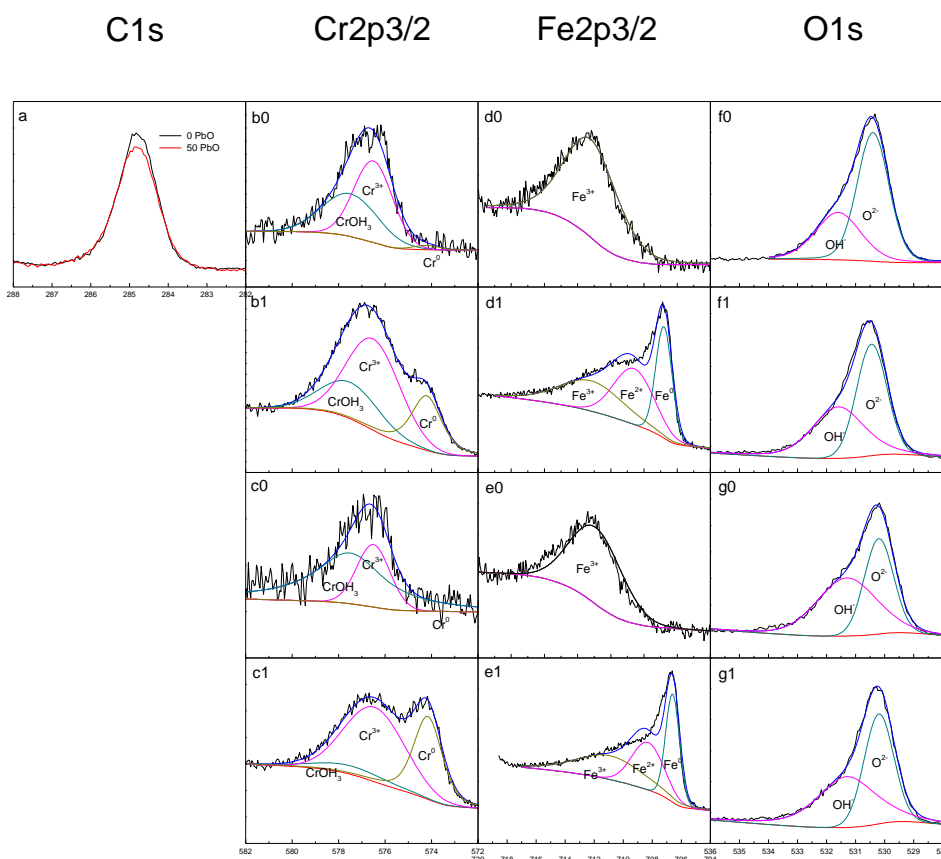


**Figure 3.** XPS spectra of the oxide film on stainless steel 304 after corroding in solutions with (b, d, and f) 0 and (c, e, and g) 50 ppb PbO addition for 120 h at 315°C: (a) C1s, (b0, b1, c0, and c1) Cr2p3/2, (d0, d1, f0, and f1) Fe2p3/2 and (f0, f1, g0, and g1) O1s at sputtering times of (b0~g0) 0 and (b1~g1) 80 s. The depth profiles were analysed by Ar<sup>+</sup> at a sputtering rate of 0.5 nm/s with a C1s peak at a binding energy of 284.8 eV.

The binding energies of Fe<sup>0</sup>, Fe<sup>2+</sup> and Fe<sup>3+</sup> moved to 706.6, 708.3 and 710.9 eV, respectively. It should also be highlighted that the binding energies of O<sub>2</sub><sup>-</sup> and OH<sup>-</sup> corresponded to 530.4 and 531.6

eV[14] of the oxide on SS304 without PbO. The two kinds of oxide substances above correspond to metal oxides and metal hydroxides, respectively. When 50 ppb PbO was added, the binding energies of  $O_2^-$  and  $OH^-$  shifted to a low direction by  $\sim 0.2-0.3$  eV, with values of 530.2 and 531.3 eV, respectively. The decreased binding energies of  $O_2^-$  and  $OH^-$  may impact metal oxide formation. According to the morphology results, less metal oxide formed during the corrosion process by trace PbO addition. Shifting of the oxygen photoelectron spectra is rare in the analysis of metals and their compounds.

#### 4. DISCUSSIONS

In general, it is considered that SCC occurs as a result of the interaction of three factors: a corrosive environment, a susceptible alloy and the presence of tensile stress [15]. However, microstructural effects and stress localization may also play a significant role. Additionally, in actual application, the reason that a very small number of ions can cause stress corrosion cracks is still unclear. In this work, the trace level presence of Pb is employed to discuss SCC from the formation of an oxide film on Ni-Fe-Cr alloys and the banding energy of each element.

The mechanism of PLSCC in Ni-Fe-Cr alloys (including stainless steel) is speculated to involve the electrodeposition of Pb on the alloy surface, either by displacement plating or underpotential deposition[16-23]. In addition, electrochemical measurements showed that Pb decreases the passive current density on Ni alloys and Ni-Fe-Cr alloys.

The binding energy changes of elements in metal oxides are caused by changes in atomic charges. The change of atomic charge played a relationship with the valence electron density and changed the outside layer of the electron cloud distributions, which reflected the chemical process of bonding, valence changes, electron density distribution, oxidation valence changes or other issues. In this experiment, the binding energies of metal oxide are decreased, which means that the average charge of the metal atom is reduced by the outer and surrounding electron shielding. The electronegativity of the atom increases, and the molecular orbital of the outer electrons becomes larger in the degree of non-localization. The stability of the metal oxide as an electron donor deteriorates. The protective properties of the oxide film on the alloy are poor/incomplete, as shown in Fig. 1. Thus, the possibility of stress cracking corrosion in the presence of a high-temperature water environment increases.

#### 5. CONCLUSION

The binding energies of  $Cr2p_{3/2}$ ,  $Fe2p_{3/2}$  and  $O1s$ , as the main protective oxide layer on alloys in high-temperature water, are decreased by trace Pb additions into the high-temperature water. This gives a result that the protective metal oxide on the alloy was diminished by the presence of Pb, which suggests a possible reason for PLSCC.

#### ACKNOWLEDGEMENT

This work was financially supported by the Natural Science Foundation of Beijing, China (2192051) and the Fundamental Research Funds for the Central Universities.

## References

1. Y.C. Lu, Comparative studies on the localized corrosion susceptibility of Alloy 690 and Alloy 800 under simulated steam generator conditions, Proceedings of the 11th International Conference on Environmental Degradation of Materials in Nuclear Power System-water Reactors, Washington, 2003, 1138.
2. S.J. Ahn, V.S. Rao, H.S. Kwon and U.C. Kim, *Corros. Sci.*, 48 (2006) 1137.
3. S.S. Hwang, U.C. Kim and Y.S. Park, *J. Nucl. Mater.*, 246 (1997) 77.
4. A. Palani, B.T. Lu, L.P. Tian, J.L. Luo, Y.C. Lu, *J. Nucl. Mater.*, 396 (2010) 189.
5. D.J. Kim, H.C. Kwon, H.W. Kim, S.S. Hwang and H.P. Kim, *Corros. Sci.*, 53 (2011) 1247.
6. B. Peng, B.T. Lu, J.L. Luo, Y.C. Lu and H.Y. Ma, *J. Nucl. Mater.*, 378 (2008) 333.
7. Y. Tan, J.H. Yang, W.W. Wang, R.X. Shi, K.X. Liang and S.H. Zhang, *J. Nucl. Mater.*, 473 (2016) 119.
8. Y. Tan, S.H. Zhang and K.X. Liang, *Int. J. Electrochem. Sci.*, 9 (2014) 728.
9. J.Q. Wang, X.H. Li, F. Huang, Z.M. Zhang, J.Z. Wang and R.W. Staehle, *Corrosion*, 70 (2014) 598.
10. Z.M. Zhang, J.Q. Wang, E.H. Han and W. Ke, *Corros. Sci.*, 53 (2011) 3623.
11. F. Huang, J.Q. Wang, E.H. Han and W. Ke, *J Mater. Sci. Technol.*, 28 (2012) 562.
12. A. Machet, A. Galtayries, S. Zanna, L. Klein, V. Maurice, P. Jolivet, M. Foucault, P. Combrade, P. Scott and P. Marcus, *Electrochim. Acta.*, 49 (2004) 3957.
13. H. Sun, X.Q. Wu and E.H. Han, *Corros. Sci.*, 51 (2009) 2840.
14. H. Sun, X.Q. Wu and E.H. Han, *Corros. Sci.*, 51 (2009) 2565.
15. D.A. Jones, Principles and Prevention of Corrosion, (1996) Pearson Education, US.
16. H. Radhakrishnan, A.G. Carcea and R.C. Newman, *Corros. Sci.*, 47 (2005) 3234.
17. X. Ru, R.W. Staehle, A theory for the role of line-contact crevices and their chemistries in promoting SCC in alloy 690, Proc. 16th Int. Conf. on Environmental Degradation of Materials in Nuclear Power Systems–water Reactors, the Minerals, Metals & Materials Society [TMS], Asheville, NC (2013), 1984-2037.
18. R. Wolfe, R. Eaker, J. Lumsden, PbSCC of alloy 690TT and alloy 800NG steam generator tubing in alkaline conditions, Proc. 16th Int. Conf. on Environmental Degradation of Materials in Nuclear Power Systems–water Reactors, the Minerals, Metals & Materials Society [TMS], Asheville, NC (2013), 1916-1934.
19. D.-J. Kim, B.H. Mun, H.P. Kim and S.S. Hwang, *Metals Mater. Int.*, 20 (2014) 1059.
20. S.W. Kim, H.P. Kim, *Corros. Sci.*, 51 (2009) 191.
21. U.C. Kim, K.M. Kim and E.H. Lee, *J. Nucl. Mater.*, 341 (2005) 169.
22. J. Lumsden, A. McIlree, R. Eaker, R. Thompson and S. Slosnerick, *Mater. Sci. Forum*, 475–479 (2005) 1387.
23. B. Capell, R. Wolfe, J. Lumsden, R. Eaker, PbSCC of alloy 800NG steam generator tubing in alkaline environments, Proc. 17th Int. Conf. on Environmental Degradation of Materials in Nuclear Power Systems–water Reactors, Canadian Nuclear Society (CNS), Ottawa, ON, Canada (2015), 713-727.